Technical Reports (CIS) Department of Computer & Information Science

October 1991

A New Range Finding Method Using a Varifocal Mirror

Chang Li
University of Pennsylvania

Xiaoping Yun
University of Pennsylvania

A New Range Finding Method Using a Varifocal Mirror

Abstract

A new range finding method is proposed in this paper which makes use of a varifocal mirror. The three-dimensional object space is first discretized into a sequence of spherical shells with a specially designed nonlinear vibrating varifocal mirror. These discrete spherical shell images are then recorded by a video camera. A deblurring algorithm is introduced in this paper which is used to remove the blurred components in the images. Different depth ranges can be obtained by controlling the vibration amplitude and the direct current component of the driving wave for the varifocal mirror. The depth accuracy is adjusted by varying the vibration period of the varifocal mirror. This range finding technique can be made real time by increasing the frame frequency of the camera.

Comments

University of Pennsylvania Department of Computer and Information Science, Technical Report No. MS-CIS-91-80.

A New Range Finding Method Using A Varifocal Mirror

MS-CIS-91-80
GRASP LAB 279

Chang Li
Xiaoping Yun

Department of Computer and Information Science
School of Engineering and Applied Science
University of Pennsylvania
Philadelphia, PA 19104-6389

October 1991

A New Range Finding Method Using A Varifocal Mirror

Chang Li* and Xiaoping Yun
General Robotics and Active Sensory Perception
(GRASP) Laboratory
Department of Computer and Information Science
University of Pennsylvania
Philadelphia, PA 19104

ABSTRACT

A new range finding method is proposed in this paper which makes use of a varifocal mirror. The three-dimensional object space is first discretized into a sequence of spherical shells with a specially designed nonlinear vibrating varifocal mirror. These discrete spherical shell images are then recorded by a video camera. A deblurring algorithm is introduced in this paper which is used to remove the blurred components in the images. Different depth ranges can be obtained by controlling the vibration amplitude and the direct current component of the driving wave for the varifocal mirror. The depth accuracy is adjusted by varying the vibration period of the varifocal mirror. This range finding technique can be made real time by increasing the frame frequency of the camera.

1 Introduction

The range finding methods in the area of machine vision can be classified into three categories: active range finding methods, passive range finding methods, and their combinations.

In the categories of active range finding methods, the ultrasonic wave, the radio wave or the microwave, the visible light, the infrared wave, as well as other form of waves are used to detect the range between the wave source and the object. All these active range finding methods emit some kind of energy towarding the object, then receive the reflected energy so that the range can be measured according to the difference of the energy transmitting time and its transmitting speed. For example, the accurate radar range finding instruments and the laser range finders belong to the active range finding methods [1] [2] [3].

The passive range finding methods use the stereo vision parallax, the phase differences, the defocus disparities, the focus information, and as well as any other disparities coming from the objects which can be used to measure the range from the viewing point to the viewed object. All these passive range finding methods only receive the energy from the objects. For example, the stereo camera range finding method and the focus range finder are well known passive range finding methods [4] [5] [6]. In some other range finding methods, the active and passive range finding methods are combined together in order to obtain some special range finding results or to satisfy some special purposes [7].

In every range finding method mentioned above, there exist some advantages and some disadvantages. For instance, although the active range finding methods can obtain more accurate range data, but they dissipate a lot of energy, and even some emitting wave is very harmful to human being. In military applications, the emitting wave can be detected by the opponent. The passive range finding methods, such as stereo range finding techniques, are

*Professor, Three-dimensional Imaging Technique Laboratory of Civil Aviation Institute of China, Tianjin, P.R.China.

very attractive to the researchers, but there are various problems which are hard to overcome, such as the stereo matching errors and the measured range accuracy [8] [9].

Facing these problems and the rapid arising requirements to three-dimensional machine vision, the researchers have to try to find the other new methods to fiding range. Recently, Pietikainen and Harwood proposed a new method to find range known as the depth from three camera stereo [10]. After Pentland's new sense for depth of field was published [5], Ma and Olsen announced their depth from zooming range finding method [11]. All these new methods of finding range make better progress in the field of three-dimensional machine vision. There will certainly be more and more new range finding methods to appear in the near future.

This paper proposes a new range finding method which makes use of the varifocal mirror. The concept of varifocal mirrors comes from a three-dimensional imaging technique which was first proposed by Muirhead in 1961 and the first three-dimensional imaging prototype was announced by Traub in 1967 [12]. Because the varifocal mirror 3D imaging technique has some attractive features which can almost display a pseudo autostereoscopic images, many researchers tried to use this method to record, transmit and display the three-dimensional pictures in broadcasting television system. Unfortunately as there exist some serious problems in varifocal mirror imaging techniques (flickering effects, ghost images, blurred pictures, etc.) which can not be solved so far, the varifocal mirror 3D imaging technique did not succeed [13] [14] [15].

However, because there are no displaying problems in three-dimensional machine vision, we can make use of the varifocal mirror as a powerful tool in range finding. First we discretize the three-dimensional object space into a sequence of the spherical shells which have the same origin. Then we do the volume scanning in this discretized 3D space and record these spherical shells separately with a specially designed varifocal mirror camera. Finally, we process these spherical images for creating a sequence of depth maps which can be used to find range. This new range finding method has some advantages:

1. it is a passive range finding method that only receive the reflecting light from the object.
2. there are no stereo matching and calibrating problems because only one camera is to be used in this method.
3. through controlling the vibration frequency of the mirror, we can obtain the different depth range and different accuracy from coarse to fine.
4. by increasing the frame frequency of the video camera, we can increase the volume scanning frequency of the varifocal mirror. Therefore, we may use this method as a real time range finding method.

2 An Introduction to Varifocal Mirror 3D Imaging Technique

A brief introduction to Traub's varifocal mirror three-dimensional imaging technique will be helpful for us to understand this range finding method.

2.1 Imaging Formula and Imaging Principle of A Varifocal Mirror

As it is well known that the image distance of an object in an optical system will be changed when the focal length of the optical system varies. Muirhead and Traub adopted this basic imaging principle in their three-dimensional imaging technique [12] [13] [14].

Let's describe how their system works. First of all, we should know the imaging function of a varifocal mirror. We consider a circular mirror with a spherical surface whose circular radius and spherical curvature radius are denoted respectively by R and r (Ref. Figure 1). According to the geometrical theory of optical imaging [16], we can derive the imaging formula of the varifocal mirror:

$$Sf_I = \frac{(R^2 + \Delta^2)(-Sf_O + \Delta)}{R^2 - 3\Delta^2 + 4\Delta Sf_O} \quad (1)$$

where Sf_I denotes the image distance, Sf_O denotes the object distance, Δ is the vibration amplitude of the varifocal mirror, and here

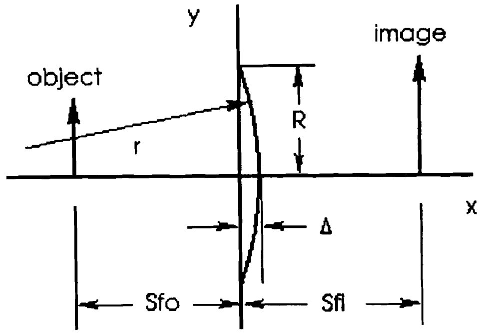

Figure 1: Imaging Principle of the Varifocal Mirror

we assume that an approximation condition $\Delta << R$ is satisfied. From the Equation(1) we can see that the image of the object in three-dimensional object space will be moving with the vibration of the varifocal mirror, so that a point in three-dimensional object space will be displayed as a three-dimensional line in image space, and a line in three-dimensional object space will be displied as a three-dimensional plane. If we arrange a series of two-dimensional pictures which contain the different depth information on a fixed object distance in the separative time sequences and control the vibration of the mirror in some order, we are supposed to see the three-dimensional images through the varifocal mirror.

Figure 2 shows how an object in three-dimensional space can be recorded, transmitted and displayed using a varifocal mirror. This method was first proposed by King and Berry in 1970 [14]. S is an object in the three-dimensional object space, VM-1 is a varifocal mirror for recording the images of the objects, BS-1 is the beam splitter which creates the virtual images of the mirror around the object plane, L is a lens which has a large aperture and short focal length and so its depth of field will be so small that only the virtual images near the object plane of the lens can be clearly recorded on the video camera, and D is the image plane of both the lens and the video camera.

While the mirror vibrating with some frequency, the virtual images of the three-dimensional objects will be moving along the optical axis of the lens, and therefore, the video camera can record a series of pictures

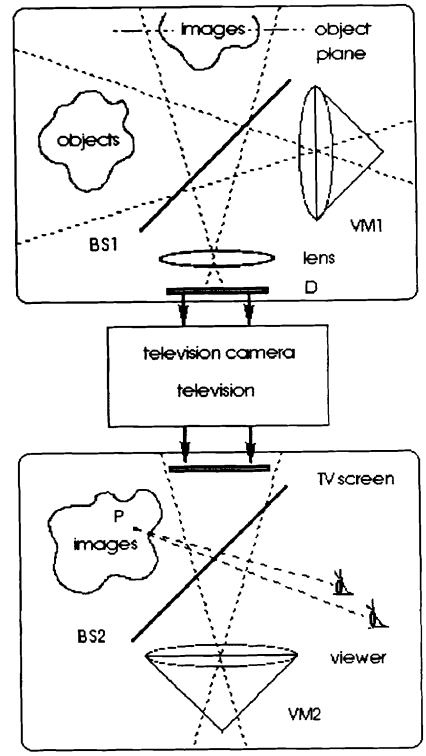

Figure 2: Recording, Transmitting, and Displaying

which contain the different depth information passing through its object plane , then all these recorded image signals are transmitted via some telecommunication means to the receiver.

At the receiver part, another varifocal mirror VM-2 which has the same specifications as the VM-1 may reconstruct the three-dimensional object images from the series of two-dimensinal pictures displayed on the television screen. The observers will see the three-dimensional effect through the beam splitter BS-2.

2.2 The Problems of A Varifocal Mirror Imaging System

We have mentioned in Section 1 that the varifocal mirror imaging system has some serious problems. Now let us explain them in details. We assume that the frame frequency of the camera is f_T, and vibration frequency of the varifocal mirror is f_V. It is obvious to see that the depth resolution of the varifocal mirror imaging system is:

$$D_R = \frac{f_T}{f_V} \tag{2}$$

For a standard TV camera, the frame frequency f_T is 25HZ, if the vibration frequency f_V of the mirror is 10HZ, we can only obtain 2.5 depth resolution. For getting a reasonable stereoscopic effects, we are not able to raise the f_V although this frequency will lead to a serious flickering and for the compatible reason of a television system we also can not raise the frame frequency of the camera. That is why we almost can not get rid of the flickering problem for the system.

As the nonlinear magnification characteristics of the varifocal mirror, a point in the three-dimensional object space will appear to the viewer although the same viewer in the object space may not see this point at all and the result is that the objects behind the opaque objects will be displayed out, and an opaque object become transparent! That is the ghost image effects of the system. Because persistence of vision, the ghost image effect can not be overcome in varifocal mirror imaging system.

Because there is a depth field of the lens, not only the virtual images just on the object plane, but also the virtual images around the object plane may be recorded on to the video camera, although these images out of the object plane are blurred. As this result, the varifocal mirror 3D imaging system can not give us the clear 3D pictures.

All these disadvantages which are very hard to be overcome hindered the varifocal mirror three-dimensional imaging technique to be used in practice. Finally, after fifteen years passed, it is almost forgot by the world.

Because there are no task to dispay a three-dimensional image on some range finding purposes, we should recall the varifocal mirror imaging technique and introduce some features of it into the range finding technical field. The following sections will express our research work in this aspect.

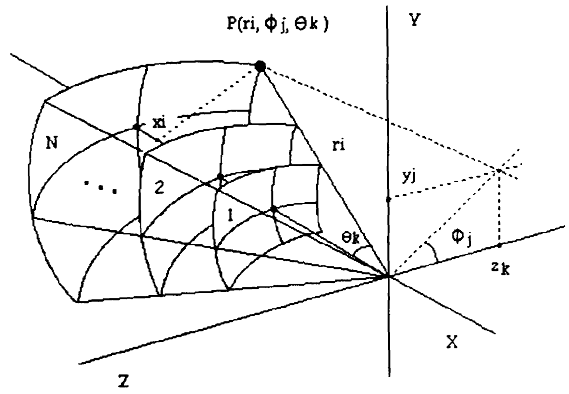

Figure 3: A Discrete 3D Object Space

3 Discretizing, Recording the 3D Objects

We break up a continuous three-dimensional object space into a discrete three-dimensional object space under a spherical coordinates and record these discrete spherical shells separately with a varifocal mirror and a video camera. For recording a linear changing distance, we must use a nonlinear driving wave to drive the varifocal mirror.

3.1 Discretizing the 3D Object Space

The later analysis will show that the three-dimensional object space is broken up into a discrete three-dimensional object space under a spherical coordinates is very convenient to derive some useful results. Let us put the optical center of a varifocal mirror on to the origin of a spherical coordinate and let the optical axis of the varifocal mirror coincide with the x axis. Figure 3 depicts the discrete situation. Assuming the area that we are interested is within:

$$\begin{aligned} r_{min} \leq \; & r_i \; \leq r_{max} \\ \phi_{min} \leq \; & \phi_j \; \leq \phi_{max} \\ \theta_{min} \leq \; & \theta_k \; \leq \theta_{max} \end{aligned} \tag{3}$$

$$\begin{aligned} i &= 1, 2, \cdots N. \\ j &= 1, 2, \cdots M. \end{aligned}$$

$$k = 1, 2, \cdots P.$$

Therefore, given every r_i, we obtain a corresponding spherical shell S_i. Through controlling the values of r_{min}, r_{max}; ϕ_{min}, ϕ_{max}; and θ_{min}, θ_{max}; we can obtain the different range area. Adjusting the number of N, we can control the depth resolution, or in other words, the range accuracy. We may perform this work through setting the definite amplitude, the direct current component of driving wave and the vibration period of the varifocal mirror.

3.2 Nonlinear Driving Wave for A Varifocal Mirror

From the introduction to the varifocal mirror three-dimensional imaging technique we have known that the video camera object plane is fixed. In order to obtain a sequence of spherical shell images which are separated by the equal intervals, we must control the moving of the virtual images in a nonlinear state. According to the geometrical theory of imaging, we can obtain the imaging function for a spherical reflecting mirror under its geometrical symmetry condition (Ref. Figure 4) as follows:

$$x_i = \frac{r_m}{2x_p - r_m} x_p$$
$$y_i = \frac{-r_m}{2x_p - r_m} y_p \quad (4)$$

where x_p, y_p is an object point on some discrete spherical shell, x_i, y_i is the image point of the object point on the image plane, and r_m is the radius of the varifocal mirror. We first square Equation(4) on both sides and add them together, then substitute $x_p^2 + y_p^2$ and $x_i^2 + y_i^2$ with R_p and R_i respectively. Introducing the approximation condition $r_m \gg x_p$, we derive another imaging formula:

$$R_i = \frac{r_m}{2R_p - r_m} R_p \quad (5)$$

Let us suppose the farest spherical shell S_N is moving towards the origin of the varifocal mirror with a constant speed V_0 and for obtaining the linear depth varies we should keep the R_i unchanged during the motion of the spherical. So we can differentiate Equation(5) and set its

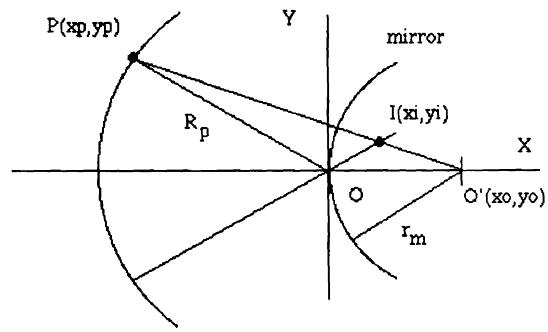

Figure 4: the Relation Between $r_m(t)$ and $R_p(t)$

derivative to be zero. Solving this equation, we obtain the relation between the linear moving of the spherical shell and the nonlinear vibration of the varifocal mirror:

$$r_m(t) = \frac{2R_i(v_0 t + R_{max})}{R_i + (v_0 t + R_{max})} \quad (6)$$
$$v_0 = \frac{R_{min} - R_{max}}{T}$$

If we keep the radius of the mirror vibration to follow Equation(6), we can record a sequence of spherical images with an equal depth interval.

A varifocal mirror can be made up in several ways and a practical method makes use of a loudspeaker on which a silver vibration film is fixed with a flange plate. The film is driven by the air within the paper basin and the paper basin is vibrated with the driving current via the speaker coil. A analysis shows that the vibration form of the film will follow the driving current wave form and if the amplitude of the mirror is not so large the film surface is almost ideally spherical. Finding the relation between $r_m(t)$ and the driving wave will be very useful in practice. Let us see Figure 5, where $r_m(t)$ is the radius of the vibrating silvering film, R_m is the radius of the speaker and $\Delta(t)$ is the vibration amplitude of the silver film. The relation between $\Delta(t)$ and $r_m(t)$ can be expressed as follows:

$$\Delta(t) = -r_m(t) + \sqrt{r_m(t)^2 - R_m^2} \quad (7)$$

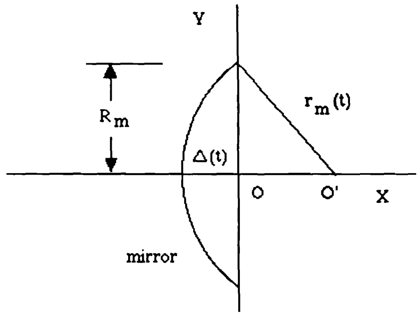

Figure 5: the Relation Between $\Delta(t)$ and $r_m(t)$

Expanding the last part of Equation(7) with a power series and omitting the higher order terms of R_m/r_m, we obtain the formula of the driving wave form for the varifocal mirror:

$$\Delta(t) = -(\frac{R_m}{2})(\frac{1}{v_0 t + R_{max}} + \frac{1}{Ri}) \quad (8)$$

$$v_0 = \frac{R_{min} - R_{max}}{T}$$

Figure 6 represents the driving wave form

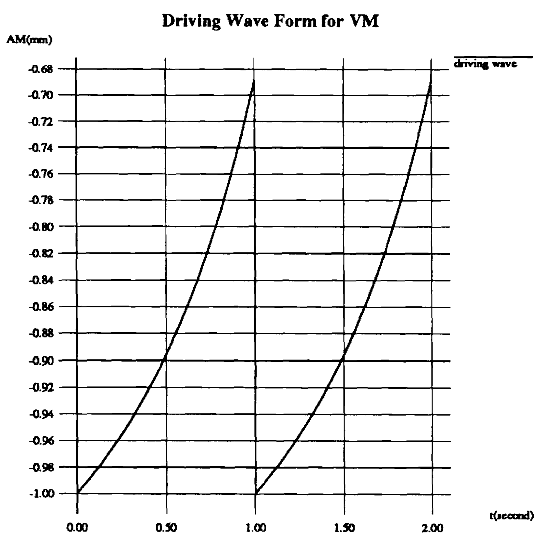

Figure 6: Driving Wave for A Varifocal Mirror

which can be easily performed by a general function generator. From Equation(8), Equation(2) and Figure 6, we obviously see that the different maximum depth ranges can be controlled by adjusting the vibrating amplitude of the varifocal mirror, and the various minimum depth ranges may be obtained

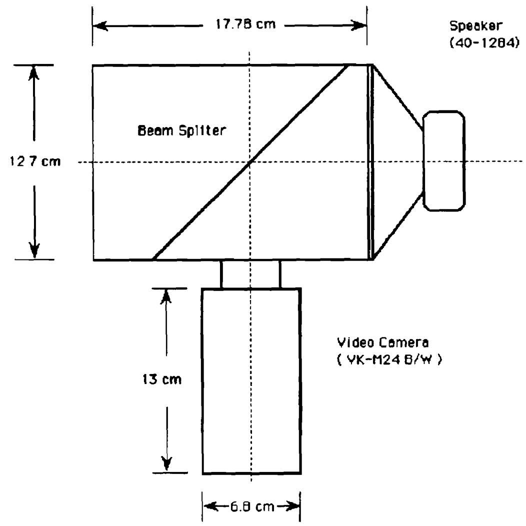

Figure 7: Structure and Specifications of A Varifocal Mirror Camera

through setting the different direct current component of the driving wave. For getting more accurate range data, we can decrease the vibration period of the varifocal mirror so that we can record more multiple spherical shells during one period and through increasing the frame frequency of the video camera we even can use this range finding method as a real time range finding technique. Figure 7 represents a practical structure and specifications of a range finding varifocal mirror camera.

4 Removing the Blurred Images

As the influence of depth field of the video camera, not only the virtual images on the object plane, but also the virtual images around the object plane will be recorded on to the video camera. To obtain a clear sequence of the discrete spherical shell images, all blurred components must be removed. There are two kinds of techniques which can be used in this task: digital deblurring method and analog filtering method. The former leads to an ideal deblurring result and the latter results in real time processing speed in spite of loosing some low frequency components of the images.

4.1 The P.S.F. of the Varifocal Mirror Camera

An optical image can be expressed as the three-dimensional convolution of a 3D object with its 3D point spread function (p.s.f.), and also a blurred image can be expressed as the result of the convolution of a 3D object with its defocus p.s.f. To remove the blurred components of the images we must know the p.s.f. with respect to the blurred images. Hopking and Stokseth discovered the properties of a defocus optical system dealing with the coherent light [17] [18]. From their research work, we can derive the infocus p.s.f. and the defocus p.s.f. under the white light condition. In the former case, the p.s.f. can be expressed as follows:

$$\begin{aligned} I(0,\nu) &= I_0 \int_{400nm}^{700nm} \frac{2J_1(\nu)}{\nu} d\lambda \qquad (9) \\ \nu &= (\frac{2\pi}{\lambda})(\frac{a_c}{f_c})r_c \\ I_0 &= (\frac{\pi a_c^2 A_o}{\lambda f_c^2})^2 \end{aligned}$$

where a_c is the radius of the video camera lens aperture, r_c is its radius variable, λ is the wavelength of light, A_o is the incident light intensity from the objects, and f_c is the video camera image distance. Figure 8 depicts the distribution of the intensity in the exact focal plane. Because the Equation(9) contains the first order *Bessel* function whose computation is very expensive, we have to find a simple function to approximate it. As is known to all, the *Gaussian* function has the similar distribution as Figure 8 and it can be proved that for any infocus point spread function in white light condition, we can find a *Gaussian* function with a definite variance σ, which can approximate the distribution of Equation(9). Figure 9 represents this approximation. In the defocus condition, we can derive the expression of p.s.f. as follows:

$$\begin{aligned} I(\mu,\nu) &= I_0 \int_{400nm}^{700nm} (\frac{2}{\mu})(U1^2 + U2^2) d\lambda \\ I_0 &= (\frac{\pi a_c^2 A_c}{\lambda f_c^2})^2 \\ U_m(\mu,\nu) &= \sum_{s=0}^{\infty} (-1)^s (\frac{\mu}{\nu})^{m+2s} J_{m+2s}(\nu) \end{aligned}$$

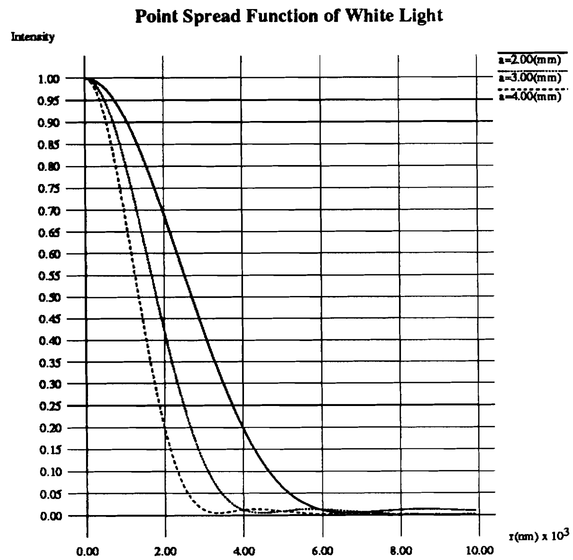

Figure 8: Point Spread Function of White Light in Focus

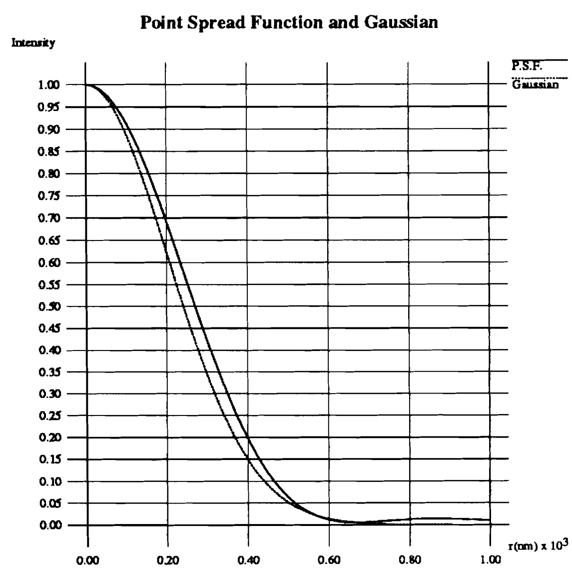

Figure 9: Approximation to P.S.F. with *Gaussian*

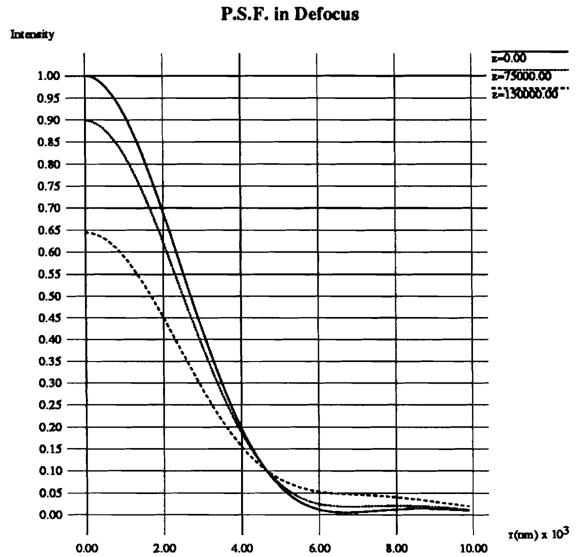

Figure 10: Point Spread Function of Defocus

$$\begin{aligned} \mu &= \frac{2\pi}{\lambda}(\frac{a_c}{f_c})^2 x \qquad (10) \\ \nu &= \frac{2\pi}{\lambda}(\frac{a_c}{f_c}) r_c \\ m &= 1,2 \end{aligned}$$

where $U_m(\mu,\nu)$ is *Lommel* function and x is defocus deviation. Although the distribution of $I(\mu,\nu)$ is so complicated that we even can not use it in practice, we also can find a *Gaussian* function with a definite variance σ as a approximate expression of Equation(10), as long as the defocus deviation x is not too large [16]. Figure 10 depicts the p.s.f. intensity distribution at different defocus. It is obvious that a definite *Gaussian* may coincide with the defocus point spread function. If we encounter some defocus images with a large deviation, we may use other more accurate approximate function to Equation(10) which can be derived from Ref. [19] [20], but the computation will be more expensive.

4.2 Deblurring Algorithm

As we described above, any optical imaging can be expressed by the convolution of a 3D object with the definite point spread functions. Referring Figure 3, 4, and Equation(5), let $p_n(r_i,\phi_j,\theta_k)$ denote a spherical image which is just positioned at the object plane of the video camera and let $h_n(r_i,\phi_j,\theta_k)$ denote the point spread function with respect to the $p_n(r_i,\phi_j,\theta_k)$, therefore, the image $g_n(y_j,z_k)$ on the video camera can be represented as follows:

$$\begin{aligned} g_n(y_j,z_k) &= h_n(r_n,\phi_j,\theta_k) \otimes p_n(r_n,\phi_j,\theta_k) \\ j &= 1,2,\cdots M. \qquad (11) \\ k &= 1,2,\cdots P. \end{aligned}$$

As the influence of depth field of the video camera, not only the spherical image on focal plane of the video camera, but also the spherical images around the focal plane will be recorded on to the video camera. Therefore, the image on the video camera at any sampled time during vibration of the varifocal mirror is a summation of responses to all spherical images. Because the vibration amplitude, the vibration frequency and the frame frequency of the video camera are all known factors, we can obtain the defocus p.s.f. in three-dimensional image space at any time sequence. Considering the blurred effect, the image on the video camera can be written out:

$$\begin{aligned} g_n(y_j,z_k) &= \sum_{i=1}^{N} h_{ni}(r_i,\phi_j,\theta_k) \otimes p_i(r_i,\phi_j,\theta_k) \\ j &= 1,2,\cdots M. \qquad (12) \\ k &= 1,2,\cdots P. \end{aligned}$$

Applying the Fourier transform to the both sides of Equation(12), and introducing the convolution theorem, we can obtain the convenient multiplication form of Equation(12) in frequency domain:

$$G_n(\mu,\nu) = \sum_{i=1}^{N} H_{ni}(\mu,\nu,\xi) P_i(\mu,\nu,\xi) \qquad (13)$$

In Equation(13), $P_i(\mu,\nu,\xi)$ is the Fourier transform of the every spherical image at the image distance r_i and do the inverse Fourier transform of $P_i(\mu,\nu,\xi)$ we can obtain the clear spherical image itself. For solving the N $P_i(\mu,\nu,\xi)$ we should have N equations which contain $N \times N$ known $H_{ni}(\mu,\nu,\xi)$ and N known $G_n(\mu,\nu)$. As we have described in preceding sections, we can record N spherical images during one period of vibration time of the varifocal mirror and the number of N can be defined by the factors of the varifocal mirror camera according to the different requirement and we also can find the definite *Gaussian* as the approximate functions of all infocus and defocus p.s.f. We substitute all point spread functions in Equations(11)(12)(13) with the *Gaussian* functions, therefore, we get the matrix equations bellow:

$$\begin{aligned} G_1 &= H_{11}P_1 + H_{12}P_2 + \cdots + H_{1N}P_N \\ G_2 &= H_{21}P_1 + H_{22}P_2 + \cdots + H_{2N}P_N \\ &\vdots \\ G_N &= H_{N1}P_1 + H_{N2}P_2 + \cdots + H_{NN}P_N \end{aligned} \quad (14)$$

From the Equation(14), we can solve the N $P_i(\mu, \nu, \xi)$, and from the inverse transform of $P_i(\mu, \nu, \xi)$, we can obtain all deblurred spherical images: $p_i(r_i, \phi_j, \theta_k)$ and where $i = 1, 2, \cdots N$; $j = 1, 2, \cdots M$; $k = 1, 2, \cdots P$.

4.3 Deblurring Method with Analog Filter

Performing the deblurring algorithm mentioned above can give out a sequence of clear images, but it will spend a lot of computing time. We can make use of the analog filtering techniques to remove these blurred images in real time speed, but some low frequency component in images will be lost.

5 Conclusion

This paper has proposed a range finding method which makes use of a specially designed varifocal mirror camera. The three-dimensional object space is discretized into a sequence of discrete spherical shells which have the definite depth range and depth interval. These discrete spherical shells are recorded respectively on to a video camera and then the blurred components are removed through a digital or an analog filtering technique. The recorded depth range and depth accuracy can be controlled by setting the parameters of the varifocal mirror system. Through increasing the frame frequency of the video camera, this range finding method can work in real time speed.

6 Acknowledgement

This research was conducted at the General Robotics and Sensory Perception (GRASP) Laboratory, University of Pennsylvania and partly supported by the National Education Committee of China and the Three-dimensional Imaging Technique Laboratory of Civil Aviation Institute of China.

We are particularly grateful to professor Ruzena Bajcsy who provided guidance throughout this research work.

We would like to thank Michael Chan and Sang W. Lee for many useful discussions and reference materials, and Filip Fuma and Helen Anderson for many helpful suggetions.

References

[1] Takeo Kanade. *Three-Dimensional Machine Vision.* Kluwer Academic Publishers, 1984.

[2] Dana H. Ballard and Christopher M. Brown. *Computer Vision.* Prentice-Hall Inc., 1982.

[3] Marc Rioux, G.Bechthold, D.Taylor, and M.Duggan. Design of a large depth of view three-demensional camera for robot vision. *Optical Engineering*, 26(12):1245–1255, December 1987.

[4] Eric Paul Krotlov. *Active Computer Vision by Cooperative Focus and Stereo.* Spriger-Verlag, 1989.

[5] Alex Paul Pentland. A new sense for depth of field. *IEEE Transactions on Pattern Analysis and Machine Intelligence*, 30(4), July 1987.

[6] David J. Fleet, Allan D. Jepson, and Michael R. M. Jenkin. Phas-based disparity measurement. *Image Understanding*, 53(2):198–210, March 1991.

[7] R. A. Jarvis. A perspective on range finding techniques for computer vision. *IEEE Transaction on Pattern Analysis and Machine Intelligence*, PAMI-5(2):569–586, September 1983.

[8] O.D.Faugeras and G.Toscani. The calibration problem for stereo. In *IEEE Computer Vision and Pattern Recognition*, pages 15–20, 1986.

[9] Hironobu Takahashi and Fumiaki Tomita. Planarity constraint in stereo matching. In

IEEE Computer Vision and Pattern Recognition, pages 446–449, November 1988.

[10] Matti Pietikainen and David Harwood. Depth from three camera stereo. *IEEE Computer Vision and Patterns Recognition*, 39(1):2–8, April 1986.

[11] Jun Ma and S.I. Olsen. Depth from zooming. *Optical Society of America A*, 1883–1890, October 1990.

[12] Alan C.Traub. Stereoscopic display using rapid varifocal mirror oscillations. *Applied Optics*, 24(5):1991–1992, September 1967.

[13] Erich G. Rawson. Three-dimensional computer generated movies using a varifocal mirror. *Applied Optics*, 7(8):1505, aug 1968.

[14] M.C.King and D.H.Berry. Varifocal mirror techniques for video transmission of three dimenssional images. *Applied Optics*, 9(9):2035, September 1970.

[15] J.Hamasaki, Y.Nagata, H.Higuchi, and M.Okada. Real-time transmission of a 3-d image using volume scanning and spatial modulation. *Apllied Optics*, 16(6):1675–1685, June 1977.

[16] M.Born and E.Wolf. *Principles of Optics*. Pergamon Press, New York, 1975.

[17] H.H.Hopkings. The frequncy response of a defocused optical system. *Proc.Roy.Soc.*, A,231, 1955.

[18] Per A. Stokseth. Properties of a defocused optical system. *Journal of The Optical Sociey of America*, 59(10):1314–1321, 1969.

[19] Kenneth R.Castleman. *Digital Image Processing*. PRENTICE-HALL,INC., New Jersey, 1979.

[20] Sarah Frisken Gibson and Frederick Lanni. Diffraction by a circular aperture as a model for three- dimensional optical microscopy. *J.Opt.Soc.Am*, 6(9):1357–1367, September 1989.